THE ASTROPHYSICAL JOURNAL, 438:650–658, 1995 January 10

NEW OBSERVATIONS WITH THE *HST* GODDARD HIGH RESOLUTION SPECTROGRAPH OF THE LOW-REDSHIFT LYMAN-ALPHA CLOUDS IN THE 3C 273 LINE OF SIGHT

RAY WEYMANN AND MICHAEL RAUCH
The Observatories of the Carnegie Institution of Washington, 813 Santa Barbara Street, Pasadena, CA 91101
ROBERT WILLIAMS
Space Telescope Science Institute, Baltimore, MD 21218
SIMON MORRIS
Dominion Astrophysical Observatory, Victoria, BC, Canada V8X 4M6
AND
SALLY HEAP
Goddard Space Flight Center, Greenbelt, MD 20771
Received 1994 March 29; accepted 1994 July 18

ABSTRACT

We present spectra of 3C 273 between 1216 and 1250 Å obtained in the (pre-COSTAR [Corrective Optics Space Telescope Axial Replacement instrument]) configuration of the GHRS, taken with the G160M grating, with a resolution of ≈ 20 km s^{-1}. The two strong Lyα lines at velocities of ~ 1000 and ~ 1600 km s^{-1} are well fitted with Voigt profiles and yield column densities, Doppler parameters and redshifts of log N(H I) = 14.19 ± 0.04, $V_{\rm Dop}$ = 40.7 ± 3.0 km s^{-1}, V = 1012.4 ± 2.0 km s^{-1}, and log N(H I) = 14.22 ± 0.07, $V_{\rm Dop}$ = 34.2 ± 3.3 km s^{-1} and V = 1582.0 ± 2.0 km s^{-1}, respectively. Motivated by the initial announcement by Williams and Schommer of detectable Hα emission associated with the ~ 1600 km s^{-1} cloud, we discuss the difficulty of finding models which can account for emission of that magnitude given the observed neutral hydrogen column density, though a recent reobservation by these authors has shown the initial detection to be spurious. The C/H abundance ratio is probably less than about one-fourth of the solar abundance in these clouds, although this result is very uncertain and model dependent.

Subject headings: quasars: absorption lines — quasars: individual (3C 273) — ultraviolet: galaxies

1. INTRODUCTION

The initial GHRS and FOS observations of 3C 273 (Morris et al. 1991; Bahcall et al. 1991) revealed a larger-than-expected number of extragalactic Lyα absorption systems. In particular, two quite strong lines were found at velocities of ~ 1000 and ~ 1600 km s^{-1}. Since 3C 273 lies at the extreme southern edge of the "southern extension" of the Virgo Cluster (Bingelli, Sandage, & Tammann 1985; Sandage, Bingelli, & Tammann 1985) and since these velocities lie in the range of Virgo Cluster galaxies, we refer to these clouds as the "Virgo Clouds" though their physical association with the cluster or any of its galaxies has not been demonstrated (Salzer 1992; Morris et al. 1993). The previous GHRS observations of the region shortward of the Lyα emission line of 3C 273 consisted of a series of six overlapping G160M exposures and one G140L exposure through the large science aperture (LSA) (Brandt et al. 1993). The shortest wavelength exposure of the G160M set began at 1235 Å. The seventh in the planned set, covering from 1215 to 1250 Å, together with additional G160M exposures of 3C 273 covering other spectral regions of special interest, was not obtained until the last week before the repair mission in 1993 December. In § 2, we report on the results of these new observations. The discussion in § 3, explores the problem of the source of the ionization of the gas posed by our observations and the level of Hα emission surface brightness initially reported from the 1600 km s^{-1} cloud by Williams & Schommer (1993; hereafter WS93). After the present paper was submitted, Dr. Williams kindly informed us that recent observations at CTIO made in 1994 April indicate that the initial detection of Hα emission reported in WS93 was spurious, as will be discussed in detail in Williams & Schommer (1994). To some extent the discussion in § 3, has thereby been rendered moot. However, we have left most of this section intact since it illustrates the constraints imposed upon models for any future detections or upper limits of Hα emission from nearby Lyα clouds. Brief discussions of the structure of the low-redshift Lyα clouds such as the one at 1600 km s^{-1} and limits on the carbon abundance are contained in §§ 4 and 5. We summarize the main results in § 6.

2. OBSERVATIONS AND REDUCTIONS

The observations reported here were obtained on 1993 November 26 and consisted of three separate integrations through the LSA using substep pattern 5, which results in pixels of $\frac{1}{4}$ diode, with each pixel corresponding to ~ 0.018 Å. Each integration was 1185 s, for a total exposure time of slightly less than 1 hour, and the grating was centered at 1232 Å.[1] The FP-Split mode was used, so that the grating was moved by ~ 5 diodes (20 $\frac{1}{4}$ diode pixels) between each of the 1185 s exposures. The spectra were reduced at the Goddard Space Flight Center using the IDL software developed by the GHRS team (Blackwell et al. 1993).

The three sets were registered with respect to one another (to offset any drifts in wavelength of the spectrograph or of the

[1] In addition, new G160M exposures have been obtained at central wavelengths of 1182, 1555 and 1651 Å. A detailed description of all the new G160M exposures, including line identifications and profile fits for all but the 1000 km s^{-1} and 1600 km s^{-1} lines, will be published elsewhere.

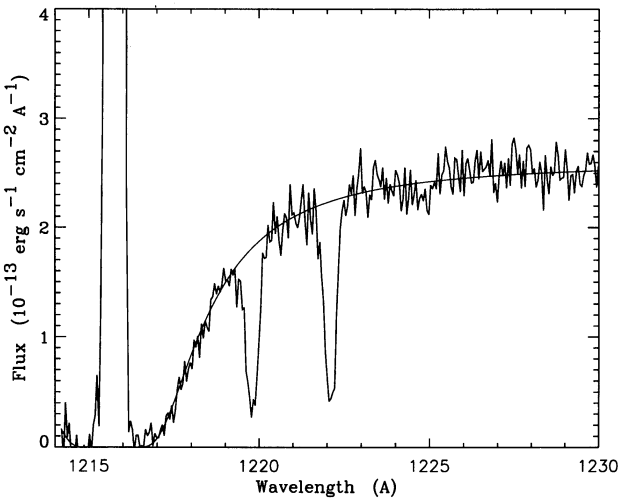

FIG. 1.—The fit to the galactic damped Lyα wing and the region of the spectrum of 3C 273 between 1215–1230 Å. The strong emission at ~1215.7 Å is geocoronal Lyα. The smooth curve defining the continuum is our best fit to the Galactic damped Lyα and yields a column density log (N_{HI}) = 20.16 ± 0.03. Weak Lyα absorption appears to be present at ~1225 Å confirming a tentative detection by Bahcall et al. (1991).

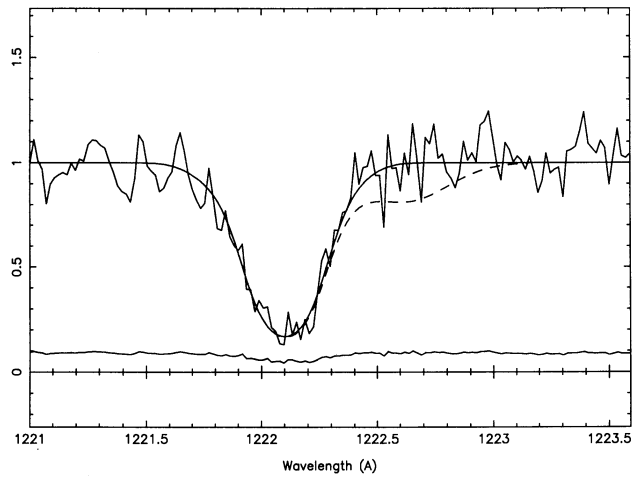

FIG. 2.—Data, 1 σ error, and Voigt profile fit to the absorption line at ~1600 km s^{-1}. The best-fitting Voigt profile to the data is shown as the smooth solid line. The dotted line shows the profile which would result from a cloud with Doppler parameter of 50 km s^{-1} and an H I column density of 2×10^{13} cm^{-2}, centered at 1713 km s^{-1}, the velocity centroid of the emission initially reported in WS93.

target in the LSA) by cross-correlating the spectra. The final S/N per $\frac{1}{4}$ diode pixel in the continuum adjacent to the 1600 km s^{-1} line is ~9. The two strong "Virgo Cloud" absorption features lie in the damping wing of the Lyα absorption produced in our own Galaxy, but at this very high resolution the slope of the damping wing is sufficiently gentle that fitting the continuum is not a serious problem. Three of us independently fitted the continuum, two of us by using high-order splines in the CONTINUUM task in ONEDSPEC in the IRAF[2] package. In the third case the continuum was fit explicitly using the analytic expression for the damping wing of Galactic Lyα and assuming the intrinsic flux of 3C 273 is constant in this region of the spectrum, which appears to be a good approximation based upon the earlier G140L results (Brandt et al. 1993). The instrumental profile was taken from Gilliland et al. (1992) and consists of a core with FWHM of ~20 km s^{-1} with extended wings. The two absorption systems were fit with the Voigt profile fitting software developed by Carswell and his collaborators (Carswell et al. 1987; Webb 1987). The data and the fit to the damped Lyα profile are shown in Figure 1. The data (with ±1 σ error arrays), and the Voigt profile fit to the 1600 km s^{-1} line are shown in Figure 2. For the two absorption lines we obtain the following results: log N(H I) = 14.19 ± 0.04, V_{Dop} = 40.7 ± 3.0, V = 1012.4 ± 2 km s^{-1}, and log N(H I) = 14.22 ± 0.07, V_{Dop} = 34.2 ± 3.3, and V = 1582 ± 2 km s^{-1}, respectively. These results are the mean for the three continuum fits described above and the probable errors include the formal ones obtained from the χ^2 fits for the individual adopted continua added in quadrature to the dispersion of the individual fits about the mean. The column density for the fit to the Galactic Lyα damping wing is log N_H = 20.16 ± 0.03. In addition to the error in this fit for the column density due to photon statistics, there is an error due to the uncertainty in the slope of the continuum of 3C 273 in the neighborhood of the galactic Lyα. The quoted uncertainty reflects our best estimate for the uncertainty due to both the photon statistics and the uncertainty in the continuum slope.

[2] IRAF is distributed by NOAO, which is operated by AURA, Inc., under contract to the NSF.

3. THE IONIZATION PROBLEM

The parameters derived above for the 1000 and 1600 km s^{-1} clouds are typical of the high-redshift Lyα forest clouds (see, e.g., Weymann 1993 for a review of their properties.) As noted there, the expectation was that direct detection of such clouds by recombination radiation would be very unlikely, since, as shown below, detection of recombination radiation from clouds with such small H I column densities requires an extremely powerful source of ionization. Thus, the initial report of Hα emission associated with the 1600 km s^{-1} cloud was unexpected (WS93). As noted in § 1, subsequent observations have shown this initial detection to have been spurious (Williams & Schommer 1994). In order to illustrate the difficulty posed for models to account for diffuse Hα emission from future possible detections along this or other lines of sight we will use the observational properties of the emission initially reported in WS93. The discussion can be modified in a fairly straightforward way to accommodate somewhat different properties.

3.1. *Photoionization Requirements*

Consider the following three basic assumptions:

1. The line of sight to 3C 273 is typical of the region over which WS93 reported the emission.
2. The ionization is due solely to photoionization.
3. The gas causing the absorption in the line of sight to 3C 273 is in ionization equilibrium.

Then, from assumptions (2) and (3), at each point along the line of sight, we have

$$n_e n_p \times R_{tot}(T_e) = \Gamma_{photo} \times n_H , \quad (1)$$

where n_e, n_p, and n_H are the electron, proton, and neutral hydrogen densities, $R_{tot}(T_e)$ is the total (electron-temperature dependent) recombination rate, and Γ_{photo} is the photoionization rate. If the entire width of the Lyα absorption were to be ascribed to thermal motion the temperature would be ~68,000

K. Since some of this width may arise from bulk motions, this temperature should be regarded as an upper limit. Typical electron temperatures resulting from photoionization are of order 20,000 K, although a gas with low metal abundance (cf. § 5) which is highly ionized by exposure to a hard radiation field may reach substantially higher temperatures. Moreover, nonradiative heating (e.g., adiabatic compression) may further heat the gas. In the following, we adopt a temperature of 40,000 K for evaluating the relevant recombination coefficients. In any case, the results depend only rather weakly on the electron temperature.

The left-hand side of equation (1) is proportional to the emission coefficient for Hα recombination radiation. Since the cloud has an opacity of only $\sim 10^{-3}$ at the Lyman limit, the ionizing flux is likely to be nearly constant along the line of sight through the cloud, so that integrating both sides of equation (1) through the cloud along the line of sight we obtain

$$S_{\mathrm{H}\alpha} = C \times N_{\mathrm{H}} \times \Gamma_{\mathrm{photo}} , \qquad (2)$$

where the surface brightness is in ergs $\mathrm{cm}^{-2}\ \mathrm{s}^{-1}$ arcsec^{-2}. Note that this relation is independent of fluctuations in density along the line of sight. Because the optical half-thickness of the slab is significantly less than one for all the higher Lyman lines and the Lyman continuum, (and only ~ 1.8 for Lyα) case A of standard nebular theory (Osterbrock 1989) is appropriate. For a temperature of 40,000 K, C for case A has the value $C \approx 6.2 \times 10^{-25}$. However, as emphasized by Ferland (1993) case A is rather artificial since for the very low optical depths implied by case A, population of the $n = 3$ level by absorption of Lyβ and higher lines of the Lyman series from the extension of the photoionization flux to the red of the Lyman limit will also be important. Rough calculations for the case of very low optical depths and a power law with a spectral index of -1 indicate that fluorescence increases the emissivity in Hα by a factor of ~ 1.7 times the case A value. (Strictly speaking, therefore, the coefficient C in eq. [2] will drop slightly as the cloud becomes optically thick, and will take on a new value appropriate for case B). For the observed column density in the 1600 km s^{-1} cloud we obtain $S_{\mathrm{H}\alpha} = 1.75 \times 10^{-10} \times \Gamma_{\mathrm{photo}}$. WS93 reported a value of 1.2×10^{-18} ergs $\mathrm{cm}^{-2}\ \mathrm{s}^{-1}$ arcsec^{-2} for $S_{\mathrm{H}\alpha}$, implying a required photoionization rate of $\Gamma_{\mathrm{photo}} = 6.8 \times 10^{-9}\ \mathrm{s}^{-1}$. WS93, recognizing that this was a very high value for an intergalactic cloud, suggested that a strong ionizing source near the Lyα cloud must be present. As discussed in Weymann (1993), the value of the mean UV background at zero redshift is still quite uncertain, but the corresponding photoionization rate probably lies in the range $1 \times 10^{-14} < \Gamma_{\mathrm{photo}} < 2 \times 10^{-13}\ \mathrm{s}^{-1}$. We now show that photoionization rates of order $6.8 \times 10^{-9}\ \mathrm{s}^{-1}$ associated with relatively isolated nearby Lyα clouds such as the 1600 km s^{-1} cloud should be directly detectable, using the specific location of the 3C 273 1600 km s^{-1} cloud as an example.

3.1.1. *Limitations on Point Sources*

Consider a point source with a power-law spectrum with a spectral index of -1 located at the center of the Virgo cluster[3] and radiating isotropically. What would be the apparent visual magnitude (as seen from Earth) of such an object if it were to provide the above photoionization rate? We obtain $m_V \approx -5.3$, i.e., brighter than Venus! A point source located much closer to the cloud could be fainter, of course. In the case of the initial WS93 report, where there appeared to be no gradient in surface brightness across the cloud over an angular extent of $\sim 7'.7$ a hypothetical point source would not likely be closer than $\sim 7'.7$ from the center of the cloud, otherwise there would be a strong gradient in Γ and hence surface brightness, across the cloud. A point source at even this close distance giving the required photoionization rate would still appear as a 4.2 mag object from Earth. A point source could be several magnitudes fainter still if it radiated as an extremely hot blackbody ($T \gg h\nu_{\mathrm{LL}}/k$), but would still have to be as bright as $m_V = 11.5$—unreasonably bright for such an unusual object. Thus, these considerations make it a priori unlikely that point sources could provide such high photoionization rates for very low-redshift Lyα clouds without being readily detectable themselves.

3.1.2. *Limitations on Diffuse Sources*

Extended diffuse sources are more difficult to rule out, but such sources producing very high-photoionization rates would also be likely to be detectable themselves. For example, in searching for nearby dwarf galaxies in the neighborhood of the 3C 273 line of sight, we have set upper limits on the surface brightness of extended objects within a radius of $\sim 8'$ of 3C 273 (Morris et al. 1993; Rauch, Weymann, & Morris 1994) of about $m_R = 26.7$ arcsecond^{-2}. Again assuming a power law with a spectral index of order -1, this implies an upper limit to the surface brightness at the Lyman limit, $J_{\nu,\mathrm{LL}}$ of order 4×10^{-21} ergs $\mathrm{cm}^{-2}\ \mathrm{s}^{-1}\ \mathrm{sr}^{-1}$. This in turn implies a photoionization rate ~ 590 times less than that required *even if such a source completely surrounded the cloud.*

3.1.3. *Evidence from the* H I *1225 Clouds*

As noted initially by Salzer (1992), the giant H I cloud, H I 1225 (Giovanelli & Haynes 1989) is at a projected separation of only ~ 200 Kpcs from the line of sight to 3C 273. Significant portions of this cloud have column densities of neutral hydrogen in excess of $10^{20}\ \mathrm{cm}^{-2}$, so that essentially all the externally incident UV photons are absorbed and converted to line photons. Consider two slabs of hydrogen, one with very large optical depth and the other with very small optical depth at the Lyman limit. Let equal amounts of collimated UV ionizing flux with spectral index -1 be normally incident on both slabs. The ratio of H I ionizing photons intercepted by the cloud with $\tau_{\mathrm{LL}} \ll 1$ to that intercepted by the cloud with $\tau_{\mathrm{LL}} \gg 1$ is $\approx \tau_{\mathrm{LL,thin}}/4$. This factor of 4 is partially offset by the factor of 1.7 due to fluorescence excitation in the thin cloud. Assume finally that the resultant Hα is radiated isotropically outward over the two surfaces, and neglect any absorption by dust.[4] (There are additional factors near unity involving the geometry assumed, the difference between case A and case B between the two clouds, as well as probable differences in electron temperatures, all of which we ignore.) Then the ratio of the Hα surface brightness from the optically thin cloud to the Hα surface brightness

[3] We adopt a distance of 16 Mpc for the Virgo cluster (and also for the distance to the 1600 km s^{-1} cloud.) The projected distance between the center of the Virgo cluster and the cloud is then ~ 2.9 Mpc, which is of course a minimum separation between the Virgo cluster and the cloud. Most of the following results depend only upon the angular separation of the Virgo cluster and 3C 273 and are independent of the assumed Virgo distance.

[4] Note that while a small amount of dust can be effective in quenching Lyα produced deep below the surface (because of the huge number of scatterings which Lyα photons undergo before escape), the same is not true of Hα photons. Some direct conversion of Lyman continuum photons into IR radiation by dust could occur, but for this to be significant the dust-to-gas ratio would have to be extremely high.

from the optically thick cloud is given approximately by $S_{H\alpha,thin}/S_{H\alpha,thick} \approx 1.7/4.0 \times \tau_{LLthin} = 0.425 \times \tau_{LLthin}$. If the flux of UV ionizing photons at the H I 1225 cloud and the 1600 km s^{-1} cloud were comparable, this would imply that the Hα surface brightness of H I 1225 should be ~2350 times that of the 1600 km s^{-1} cloud. In fact, weak Hα emission due to a small dwarf galaxy is seen in the NE concentration of H I 1225, but none in the SW concentration (Salzer et al. 1990; Rauch et al. 1994.) Although the sensitivity was not as great as that obtained by WS93, the observations of Rauch et al. (1994) set a 3 σ upper limit on the Hα surface brightness in the SW component of 1×10^{-17} ergs cm^{-2} s^{-1} arcsec^{-2}, only ~8 times greater than the WS93 value, compared to the required factor of ~2350.

The foregoing argument is obviously specific to the case of the 1000 and 1600 km s^{-1} clouds in the 3C 273 line of sight, but could be applied to any situation in which a Lyα cloud is in the general vicinity of an H I cloud with large optical depth in the Lyman continuum. More generally, the considerations of §§ 3.1.1, 3.1.2, and 3.1.3, illustrate the difficulty of accounting for the high photoionization rates which would be required for detecting Hα emission from a low-redshift Lyα cloud with typical column density $\sim 10^{14}$ cm^{-2} provided all three of the assumptions enumerated at the beginning of § 3.1 hold. Before proceeding to consider the consequences of dropping one or more of these assumptions however, it is of interest to estimate what contribution to the photoionization rate *known* sources in the Virgo cluster make to the low-redshift clouds in the 3C 273 sightline.

3.1.4. *Expected Photoionization Rate from Virgo Cluster Sources*

We consider three sources: (1) the flux from the thermal bremsstrahlung associated with the Virgo Cluster extended X-ray source. (2) The nonthermal UV flux from the core and jet of M87, and (3). The UV flux from galaxies in the Virgo cluster.

1. *Photoionization rate by X-rays from the Virgo Cluster.*—The mean intensity from the extended X-ray source in the Virgo Cluster centered on M87 is given by

$$J_\nu = \tfrac{1}{2} \int_0^\theta S_\nu(\theta') \sin\theta' \, d\theta' , \qquad (3)$$

where θ is the angular extent of the Virgo cluster in X-ray emission as seen from the Lyα cloud, and S_ν is the surface brightness as a function of frequency and θ.

For simplicity it was assumed that the X-ray surface brightness in Virgo is spherically symmetric, with the radial dependence taken from the southern half of the plot of surface brightness versus θ given by Takano et al. (1989), who plot the surface brightness in a 1.5–5.4 keV band. Significant emission extends out to ~3° from M87, with detectable emission extending to ~6°. Seen from a Lyα cloud at the same distance from us as the Virgo Cluster, 6° corresponds to an angular extent of radius $\theta \sim 30°$. We assume a bremsstrahlung spectrum with temperature 2.4 keV. (The photoionization rate from the power-law spectrum originating in the core and jet of M87 itself is considered below.) In evaluating the photoionization rate

$$\Gamma = \int_{\nu_{LL}}^{\infty} \frac{4\pi J\nu}{h\nu} \alpha(\nu) d\nu , \qquad (4)$$

we chose an upper limit of 1 keV for the integration and included the effect of secondary collisional ionizations by photoelectrons with X-ray energies, both from H and He photoionizations, following Silk & Werner (1969). We adopt their parameterizations of the cross sections given by Bell & Kingston (1967) and obtain $\Gamma_{Xray} \approx 3 \times 10^{-17}$ s^{-1}.

2. *The nucleus in M87.*—We use the compilation of Biretta et al. (1991) for the fluxes from the core and knots in the jet of M87. We summed their fluxes from the core and knots in the jet in the *g*-band and assumed a mean spectral index of 1.25 from the *g*-band through the ultraviolet and into the soft X-ray region. The resultant photoionization rate at the cloud [assuming as always a distance ratio Earth-Virgo/Virgo-cloud of ≈(16/2.9) = 5.5] is $\Gamma_{M87} \approx 2.5 \times 10^{-17}$ s^{-1}. This calculation assumes that there is no enhancement of the flux radiated toward the cloud due to beaming. Since the angle between the M87 jet and the direction toward 3C 273 is not far from 90° (≈113°) it seems unlikely that significant beaming occurs.

3. *The UV flux from galaxies in the Virgo cluster.*—We consider, in fact, only the UV flux from early-type galaxies. Recently, Ferguson et al. (1991) published results of *HUT* far-UV observations of the giant elliptical NGC 1399. They concluded that the spectral energy distribution between 1050 Å and the Lyman limit is dominated by stars with temperatures less than 25,000 K, and that a model atmosphere with T_{eff} = 24,000 K and log (*g*) = 4.0 is not a bad fit to the data over their observed spectral coverage. Previously, Burstein et al. 1988 presented *IUE* data on several early-type galaxies, including several in the Virgo cluster. They present data relating the flux in a band centered at 1550 Å to that in the *V* band. Finally, Sandage et al. (1985) present data on the luminosity functions of both early- and late-type galaxies in the Virgo cluster. The integrated *B*-band luminosity of the E and S0 galaxies is equivalent to a single 6.96 mag object. Using a mean $(B-V)$ of 0.95 this implies a *V* magnitude of ~6.0, or, as seen from the cloud, a *V* magnitude of 2.3. The mean $(V-\lambda 1550)$ index for the Virgo objects observed by Burstein et al. (1988) is 3.16, implying a 1550 Å flux at the cloud of $4\pi J_\nu \approx 2 \times 10^{-23}$ ergs cm^{-2} s^{-1} Hz^{-1} sr^{-1}. Integrating over a model atmosphere characterized by T_{eff} = 24,000 K and log (*g*) = 4.0 with this flux at 1550 Å results in $\Gamma_{Virgo(E+S0)} \approx 4 \times 10^{-18}$ s^{-1}.

For comparison, the photoionization rate associated with the estimate of Madau (1992) for the metagalactic background at zero redshift due to QSOs is $\Gamma_{QSOs} \approx 1.6 \times 10^{-14}$ s^{-1}. It is probably safe to conclude therefore that these three local sources in the Virgo cluster do not significantly enhance the photoionization rate due to the background QSOs. However, the very low rate for the Virgo early-type galaxies is largely due to the huge Lyman discontinuity associated with the T_{eff} = 24,000 K models. The estimate of Sandage et al. 1985 for the integrated *B* magnitude of spirals shows that they contribute a comparable amount of flux in the *B* band as do the ellipticals. Obviously, spirals and irregulars could contribute to a photoionization rate orders of magnitude larger than our estimate for the ellipticals. While uncertain estimates for the number of ionizing photons generated in late type galaxies can be made, at present the uncertainty in the fraction of ionizing photons which escape without being absorbed by local gas is still very large, even for our own galaxy. Indeed limits on the flux of ionizing photons incident on the H I 1225 cloud may provide the most useful limit on this fraction (Vogel et al. 1994).

3.2. *Fluctuations in Column Density along Neighboring Lines of Sight*

We now consider the consequences of dropping the first of the three basic assumptions (the line of sight through the absorbing cloud to the background QSO is typical of the region over which Hα emission is detected) while retaining the

other two, and examine whether we can plausibly explain observable levels of surface brightness in Hα without having to invoke a source of ionizing radiation as powerful as that required in §§ 3.1.1 and 3.1.2.

The following parameters are again specific to the WS93 announcement but illustrate the constrains on models to explain possible future detections. If a significant portion of the ~7.7 diameter region over which WS93 reported emission had a much higher column density than the line of sight to 3C 273, then the requirements for the ionizing flux would be eased considerably. However, this cannot be realized by a large-scale strong gradient in the H I column density, otherwise this would result in a corresponding strong gradient in the Hα surface brightness. We must therefore invoke instead a large number of very small cloudlets with large H I column densities, whose scale is so fine that the surface brightness fluctuations would not be apparent in typical Fabry Perot observations. If η is the mean number of cloudlets in the line of sight in the neighborhood of the QSO line of sight, then η must not be $\gg 1$, otherwise it is very unlikely that the line of sight to the QSO would avoid one of the hypothetical high H I column density cloudlets. On the other hand, since the fraction of the area covered by the cloudlets is $1 - e^{-\eta}$, if η were $\ll 1$, each cloud would have to have a surface brightness which was higher by a factor of $1/\eta$ times the average surface brightness. This requires in turn an intense radiation field even for high column density clouds, and vitiates the rationale for this model. Moreover, the observations of Morris et al. 1993, taken with a series of narrowband filters, set 3 σ upper limits of $\sim 6 \times 10^{-18}$ ergs cm^{-2} s^{-1} arcsec^{-2} on the fluctuations in the Hα surface brightness in the vicinity of the 3C 273 line of sight. Thus, unless the scale of the fluctuations in surface brightness were very small—less than ~2″ (~160 pc at the adopted distance of 16 Mpc)—these fluctuations would have been seen for $\eta \lesssim \frac{1}{3}$. Consider $\eta = 0.5$, which requires a mean surface brightness from each cloudlet of ~2.5 times the mean surface brightness or 3.0×10^{-18} ergs cm^{-2} s^{-1} arcsec^{-2}. If the cloudlets were to each have extremely high column densities ($\tau_{LL} \gg 1$) then, following the discussion in § 3.3.1 the requirements on the photoionizing intensity would be reduced by a factor of ~2350/2.5 ~ 1000. But the integrated effect of such high column densities would look like a giant H I cloud, and would have been detected by 21 cm measurements (van Gorkom et al. 1993). H I column densities lower than $\sim 10^{19}$ would perhaps not be detected, but the required photoionizing flux increases rapidly once the H I column density drops much below this.

As one can see from the discussion in § 3, even a reduction in the required ionizing flux by ~1000 still requires unreasonably bright point sources, although we cannot exclude very local diffuse sources under these circumstances.

Although we cannot definitely exclude such models for low-redshift Lyα clouds, a swarm of optically thick cloudlets with covering factor of order unity seems excluded for the *high*-redshift Lyα clouds. For example, in observations of close pairs (e.g., Smette et al. 1992) a strong correlation is observed between the equivalent widths of lines at a given redshift along two lines of sight. This can be interpreted as arising from either single large clouds with sizes large compared to the line of sight separation or else swarms of large numbers of small clouds along each line of sight. However, if the number of clouds along each line of sight were constrained to be of order unity, then one of the lines of sight should sometimes pass through a cloudlet while the other one misses a cloudlet, leading to very large fluctuations in the ratio of equivalent widths. Such large fluctuations are not observed. Of course, it is quite possible that the low-redshift Lyα clouds are of a wholly different character than the high-redshift Lyα clouds, so this latter argument is not a strong one.

3.3. *Collisional Ionization*

We next consider dropping assumption (2)—that the ionization is due to photoionization. In particular, we consider the possibility that the ionization is due to (thermal) collisional ionization. We first consider a uniform slab of hot gas without regard to the possible origin of the heating and will take the highest possible temperature allowed by the observations, namely 68,000 K, corresponding to a Doppler parameter of 34 km s^{-1}. We shall use this temperature in the following estimates of the collisional and recombination rates. At what density would collisional ionization dominate over photoionization? Suppose, as we have suggested above, that local sources (e.g., in the Virgo cluster) contribute at most a comparable amount of ionizing radiation to the value averaged over large volumes of space at zero redshift. There have been several attempts to measure or estimate the value of the "metagalactic" ionizing flux at zero redshift. As discussed in Weymann (1993; see also Kulkarni & Fall 1993) we regard some of these as upper limits, while the estimate of Madau (1992) is probably a lower limit, since it considers only QSOs and AGNs as the source of the UV radiation. For a power law with spectral index -1, we may characterize the background by the value of J_ν at the Lyman limit, and a value $J_{\nu,LL} \approx 2 \times 10^{-23}$ ergs cm^{-2} s^{-1} sr^{-1} seems a reasonable estimate. Using collisional ionization rates kindly provided by R. Sutherland and M. Shull we have $C_{ion} \approx 1.6 \times 10^{-9}$ cm^3 s^{-1} for T = 68,000 K.

For the radiation field assumed above, collisional ionization dominates over photoionization for electron densities $n_e > 3.9 \times 10^{-5}$. Thus, for electron densities significantly above this value, the level of ionization will be set by collisional processes alone and hence independent of density. The fraction of neutral hydrogen is then $n_H/n_p \approx 5.9 \times 10^{-5}$. The observed neutral hydrogen column density and the observed Hα surface brightness then imply the two conditions

$$\int n_p \, dl \approx 2.7 \times 10^{18} \text{ cm}^{-2} , \tag{5}$$

$$\int (n_p)^2 \times dl \approx 2.4 \times 10^{19} \text{ cm}^{-5} , \tag{6}$$

where it has been assumed that $n_e \approx n_p$. (Collisional excitation of Hα has been ignored, but it does not change the order of magnitude of these relations.)

In contrast to the discussion in § 3.1 where photoionization equilibrium was assumed, the size, geometry, and distribution of material along the line of sight is important. If one imagines the material concentrated in a uniform sheet whose normal is along the line of sight, then for the above two equations to be satisfied requires $n_p \approx 10$ cm^{-3} and a thickness, L, of only $L \approx 2 \times 10^{17}$ cm. The required thickness scales as $1/x^2$ (where x is the fraction of hydrogen that is neutral), and the required electron density directly with x.

High levels of ionization require higher temperatures which might be achieved by shocks. Models for Lyα clouds involving cooling gas behind shock fronts were in fact considered by Hogan (Hogan 1987), although not, of course with the con-

straints on Hα surface brightness and H I column density considered here. Before considering this possibility however, one additional interesting discrepancy between the initial WS93 surface brightness observations and the spectroscopic absorption observations should be noted: WS93 found a value of $V = 1713 \pm 4$ km s^{-1} for the center of the emission. We measure a (heliocentric) central velocity of 1582 ± 2 km s^{-1} for the Lyα absorption line. At the Hα emission this difference of 131 km s^{-1} corresponds to a blue shift of ~ 2.9 Å from the center of the emission. One interpretation of this velocity difference between the Hα emission and the H I absorption might have been a feature associated with the dynamics of the shock structure. In another sense, however, this velocity difference makes the problem even more difficult, since reference to our Figure 2 shows no absorption displaced by this velocity (~ 0.5 Å) toward the red. Moreover, the Hα emission seemed to be unresolved at the instrumental resolution of WS93, and thus would have had to have a Doppler parameter which did not exceed ~ 50 km s^{-1}. This implies that the gas responsible for the bulk of any emission could not have been hotter than $\sim 150{,}000$ K, so if it was initially at a much higher temperature *it must have cooled.* We use this cooling constraint in the discussion below. A reasonable upper limit on the column density of neutral hydrogen centered at this velocity, even with a Doppler parameter of 50 km s^{-1} (corresponding to $T \approx 150{,}000$ K) is $\sim 3 \times 10^{13}$ cm^{-2}. (See Fig. 2.)

3.3.1. *Quasi-stationary One-dimensional Shocks*

To investigate shock models definitively requires rather specific scenarios involving detailed (2D or 3D) hydrodynamic calculations, which are beyond the scope of this paper. Instead we consider plane-parallel flows behind shocks, with the flows assumed steady in the shock frame. The shocks might arise as the result of two colliding clouds of gas with relative velocity $v_{\rm rel}$ and preshocked particle density n_0. We assume a strong shock with $v_{\rm rel}$ sufficiently high and/or the preshocked gas already ionized so that we neglect ionization energy in the shock conditions. Then

$$T_{\rm shock} \approx 6.0 \times 10^4 \text{ K} \times (v_{\rm rel}/100 \text{ km s}^{-1})^2$$

with the incoming velocity in the shock frame, $v_{\rm shock} \approx \frac{2}{3} v_{\rm rel}$. If the shocked gas is heated above $\sim 10^5$ K, then it must have had time to cool in order that the emission width not be greater than the upper limit adopted above. For a strong shock, the pressure is nearly constant as the gas cools. The detailed temperature and ionization structure behind a cooling shock which is steady in the rest frame of the shock has been studied by a number of authors (see, for example Schmutzler & Tscharnuter 1993 and references therein.) They show that not until the temperature has dropped to $\sim 20{,}000$ K does the ionization of the hydrogen depart significantly from the (collisional) equilibrium value at any temperature. Using their results for a very low metal abundance gas, one can evaluate the Hα emissivity and the H I column density accumulated downstream from the shock as a function of the shock velocity, $v_{\rm shock}$, preshock density n_0, and the point downstream at which the gas has cooled to some temperature T. (Since for a given shock velocity and down stream temperature both the cooling length and column density scale as $1/n_0$ the H I column density is independent of the preshock density; cf. Hogan 1987.) The result is that for shock temperatures much above $T_{\rm shock} = 10^5$ K, H I column densities in excess of 3×10^{13} cm^{-2} (our limit on the H I column density centered at the velocity of the Hα emission initially reported in WS93, and a typical upper limit which GHRS G160M observations can place on fairly broad, weak Lyα absorption) are built up before the gas has had a chance to cool. For $v_{\rm rel} = 125$ km s^{-1} and $T_{\rm shock} \approx 10^5$ K, a column density of $\log N(\text{H I}) = 13.5$ is reached when the shock has cooled only to $T = 70{,}000$ K. In order for this segment of the cooling shock to produce Hα emission at the WS93 level, the preshock density would have to be of order 6 cm^{-3}. Radiation from the shock itself is not nearly sufficient to prevent the shock from cooling further. Since the cooling and recombination times are very short—less than 1000 yr—it seems almost inevitable that unacceptably large H I column densities would result.

To summarize: It seems very difficult for shock models to produce Hα emission at the WS93 level, at temperatures which are also cool enough so as not to produce emission line widths which are readily resolved with Fabry Perot interferometers, without at the same time producing prohibitively large neutral hydrogen column densities. In principle, the gas could also cool adiabatically if $t_{\rm expan} \sim R_{\rm cloud}/v_{\rm rel} \ll t_{\rm cool}$. However, the expansion would then rapidly quench the emission. Moreover, much of the thermal energy would be converted back to bulk motion resulting in large emission widths.

While we have certainly not explored all possible models which could account for both diffuse Hα surface brightness at levels comparable to WS93 and the very low H I column densities seen by GHRS and FOS, finding plausible models appears to us to pose a difficult problem.

4. STRUCTURAL PROPERTIES

We now consider a very simple version of a currently popular model for the *high*-redshift Lyα clouds: Namely, gas spheres, the inner regions of which may be considered isothermal clouds in hydrostatic equilibrium, with possible contributions to the gravitational potential from dark matter. We further assume that the effective velocity dispersion of both the hydrogen and the dark matter are the same. We also assume that the measured Doppler parameter is an indicator of the effective pressure support of the gas, regardless of whether thermal motions or "microturbulence" dominate. We define a characteristic radius $R_{1/2}$ such that the surface brightness along a ray with impact parameter $R_{1/2}$ has $\frac{1}{2}$ the surface brightness of a ray passing through the center. If the gas is in photoionization equilibrium, then from equation (2) it follows that along this ray the neutral hydrogen column density is also $\frac{1}{2}$ of its value along a ray through the center.[5] Carrying out the appropriate integrations for an isothermal structure we obtain

$$R_{1/2} = 93 \times V_{34} \times (n_{-4} \times f)^{-1/2} \text{ kpc}\,, \qquad (7)$$

where V_{34} is the Doppler parameter in units of 34 km s^{-1}, n_{-4} is the central density of protons in units of 10^{-4} and f is the ratio of dark matter to baryon mass density. (Here and below we assume the presence of fully ionized helium with number density ratio $n_{\rm He}/n_{\rm H} = 0.1$.)

In order to illuminate the constraints which would be set on the structure by detectable levels of Hα surface brightness, we will consider two cases in parallel: The "S" case, in which we assume Hα surface brightness at levels comparable to that reported in WS93, and the "J" case, in which we assume a

[5] If the ionization in the cloud is dominated by collisions, then the neutral hydrogen column density will not scale with the Hα surface brightness and will have dropped to only ≈ 0.75 of its central value at $R_{1/2}$.

value for the mean intensity of the background radiation field, with the gas in photoionization equilibrium with this radiation field (assumed to have a spectral index of -1). We denote the neutral hydrogen column density along a line of sight with impact parameter $R_{1/2}$ by $N_{\rm H14}$, measured in units of 10^{14} cm^{-2}. As before, we assume an electron temperature of 40,000 K in computing the Hα emissivity. For the "S" case, we interpret the Hα surface brightness as the mean value inside the projected disk of radius $R_{1/2}$. For the "J" case, the cloud properties are a function of the Doppler parameter and the product of the neutral hydrogen column density, $N_{\rm H14}$, and background radiation field, J_{-23}, where J_{-23} is the mean intensity at the Lyman limit in units of 10^{-23} ergs cm^{-2} s^{-1} hz^{-1} sr^{-1}.

For the "J" case:

$$
\begin{aligned}
R_{1/2} &= 526 \times V_{34}^{4/3} \times f^{-2/3} \\
&\quad \times (N_{\rm H14} \times J_{-23})^{-1/3} \text{ kpc}, \\
M_{\rm tot(1/2)} &= 5.1 \times 10^{10} \times V_{34}^{10/3} \times f^{-2/3} \\
&\quad \times (N_{\rm H14} \times J_{-23})^{-1/3} M_{\odot}, \\
n_{\rm central} &= 3.1 \times 10^{-6} \times V_{34}^{-2/3} \times f^{1/3} \\
&\quad \times (N_{\rm H14} \times J_{-23})^{2/3} \text{ cm}^{-3}, \\
M_{\rm H\,I(1/2)} &= 9.8 \times 10^{5} \times V_{34}^{8/3} \times f^{-4/3} \\
&\quad \times (J_{-23})^{-2/3} \times N_{\rm H14}^{1/3} M_{\odot}. \qquad (8)
\end{aligned}
$$

Here, $M_{\rm H\,I(1/2)}$ is the *projected* mass of neutral hydrogen within a disk of radius $R_{1/2}$.

For the "S" case, from the considerations in § 3, the cloud properties scale as follows, where S_{-18} denotes the Hα surface brightness in units of 10^{-18} ergs cm^{-2} s^{-1} arcsec^{-2}, and where it has been assumed that recombination radiation at a temperature of 40,000 K is the only contributor to the Hα surface brightness.

$$
\begin{aligned}
R_{1/2} &= 7.4 \times V_{34}^{4/3} \times f^{-2/3} \times S_{-18}^{-1/3} \text{ kpc} \\
M_{\rm tot(1/2)} &= 7.3 \times 10^{8} \times V_{34}^{10/3} \times f^{-2/3} \times S_{-18}^{-1/3} M_{\odot} \\
n_{\rm central} &= 1.6 \times 10^{-2} \times V_{34}^{-2/3} \times f^{1/3} \times S_{-18}^{2/3} \text{ cm}^{-3} \\
M_{\rm H\,I(1/2)} &= 198 \times V_{34}^{8/3} \times f^{-4/3} \times S_{-18}^{-2/3} \times N_{\rm H14}^{1/3} M_{\odot} \qquad (9)
\end{aligned}
$$

(The coefficient given for $M_{\rm H\,I(1/2)}$ in the "S" case assumes photoionization dominates; if collisions dominate in setting the ionization the coefficient becomes 160.)

In the "J" case structures, the absence of dark matter and a value for the column density of H I equal to the observed value lead to huge structures which are likely to be vulnerable to tidal and ram pressure disruption. A ratio of dark matter mass to baryon mass, $f \approx 20$ produces structures which are not quite so large and massive. Additionally, in the "J" case we have no a priori reason to assume that the observed line of sight passes close to the center of the cloud, so that the value of the H I column density at the $R_{1/2}$ parameter could be significantly larger than the observed value, leading to still more compact and less massive structures. For central H I column densities much higher than $\sim 10^{17}$ cm^{-2} self-shielding will occur and the structures should then become visible in 21 cm, as in the case of the H I 1225 cloud. Even with a 20/1 mass ratio of dark matter to baryons and an H I column density of $\sim 10^{17}$, the mass of the structure is still considerable—about $7 \times 10^{8} M_{\odot}$.

In the case of the "S structures" where some unspecified source produces the ionization leading to observable recombination radiation, the situation is quite different: the clouds must be much denser and smaller. In fact, for a 20/1 mass ratio of dark matter to baryons, the scale length is only ~ 1 kpc. This scale would subtend an angle which is easily resolvable for low-redshift clouds and would be accompanied by a strong gradient in surface brightness on that scale.

5. CARBON ABUNDANCE LIMITS

As noted in the footnote in § 2, in addition to the exposure covering the "Virgo" Lyα absorption systems described above, we obtained additional G160M exposures including one centered at ~ 1555 Å. The purpose of this exposure was to obtain improved limits on the C IV counterparts to the two Lyα lines at 1000 and 1600 km s^{-1}. (This spectrum and a description of the data will be published elsewhere.) We make two assumptions about the Doppler parameter of these C IV systems: (1) They have the same Doppler parameter as the Lyα lines themselves (i.e., the line width is dominated by macroscopic motions) and (2) They have a Doppler parameter of $1/(12)^{1/2}$ of the Lyα lines (≈ 10 km s^{-1}; i.e., the line width is mostly thermal). Convolving each of these two cases with the instrumental PSF and running several trial column densities, we believe that a conservative upper limit for the C IV column density is about a factor of 10 lower than the H I column densities, i.e., $\sim 2 \times 10^{13}$ cm^{-2} for both the 1000 and 1600 km s^{-1} systems assuming a 34 km s^{-1} Doppler width and 1.5×10^{13} cm^{-2} assuming 10 km s^{-1} widths. We adopt the more conservative value (2×10^{13}) as the upper limit on the C IV column density in the following discussion.

To estimate the levels of hydrogen and carbon ionization which might be expected if only the expected level of the intergalactic background radiation is present, we ran a series of ionization models using CLOUDY (Ferland 1993.) The results depend of course not only upon the electron density and intensity of the radiation field at the Lyman limit, but also upon the shape of the radiation field, especially beyond the ionization potential of C^{++} at ~ 3.5 Ry. We experimented with both the "standard AGN" and "background" (at $z = 0.0$) options in CLOUDY for specifying the shape of the radiation field. In both cases the intensities were adjusted so that the specific intensity, J_{ν}, at the Lyman limit was 2×10^{-23} ergs cm^{-2} s^{-1} Hz^{-1} sr^{-1}. We considered slabs with constant density and varied the ionization parameter by varying this density. We can equally well characterize these sequences by specifying the thickness of the slab required to produce the observed H I column density of the 1600 km s^{-1} cloud. At high densities ($\gtrsim 10^{-3}$), more of the carbon is in the form of C II than C IV. At this level of ionization there is a sufficient amount of neutral hydrogen present that no interesting limits on the C/H abundance can be set from the C II λ1334 line (Morris et al. 1993); moreover at such densities a cloud thickness of only ≈ 100 pc would produce the observed column density.

For the "background" shape a broad maximum in the ratio of (C IV/$C_{\rm tot}$)/(H I/$H_{\rm tot}$) occurs which has a value of ~ 2000 at a particle density of $\sim 3 \times 10^{-5}$ cm^{-3}. Over the range of ionization for which this ratio is at least half this maximum, the required thickness of the cloud varies from ~ 1.5 kpc to ~ 500 kpc. If we accept these two values as plausible limits between which the actual cloud thickness lies, then (C IV/$C_{\rm tot}$)/($H_{\rm tot}$) $\gtrsim$ 1000. Combined with the limits on the C IV column density described above, we can thus only infer that log [C/H] does not exceed ~ -4, i.e., about one-fourth the solar abundance. The "AGN" shape produces substantially more C IV for a given ratio of (H I/$H_{\rm tot}$) than the "background" shape and the

ratio (C IV/C_{tot})/(H I/H_{tot}) continues to rise monotonically as the particle density is lowered past the point where the required slab thickness is becoming unreasonably large—e.g., ~ 1 Mpc. As the log of the particle density is varied from -4.0 down to -5.0, corresponding to required slab thicknesses which vary from ~ 1.5 kpc to ~ 150 kpc, log [(C IV/C_{tot})/(H I/H_{tot})] increases from 3.12 to 3.83, corresponding to upper limits on log [C/H] which decrease from ~ -4.1 to ~ -4.8.

Much more stringent limits on the C/H ratio have recently been obtained by Tytler & Fan (1994) for *high* redshift Lyα lines of comparable strength by co-adding portions of high-resolution spectra in HS 1946+7658 corresponding to the expected positions of the C IV lines from 65 Lyα systems. As and when comparable *HST* data become available it will clearly be of interest to do the same. However, determination of both the intensity and shape of the ionizing flux at low redshifts, as well as the characteristic sizes of the clouds, will also be necessary before reliable abundance limits can be set on the nearby low redshift low column density Lyα clouds.

6. SUMMARY

We have presented GHRS 160M spectra of 3C 273 covering the region from 1216–1250 Å. We derive Doppler parameters and column densities for the two strong Lyα absorption lines at 1000 and 1600 km s^{-1}. We explored various scenarios for reconciling our H I column density measurements of these clouds with Hα surface brightnesses at levels initially reported by WS93 (which they suggested was associated with the 1600 km s^{-1} absorber.) We estimate the brightness of various hypothetical point and diffuse sources of ionization and observational limits which can be placed on such sources (§ 3.1) and find that they are quite unlikely. Models invoking small dense clouds (and which are missed by the line of sight to the background QSO) would have to lie in very small regions of covering factor and column density parameter space and still require rather intense sources of ionizing photons (§ 3.2). Processes relying on collisional ionization would require very thin dense hot sheets, such as might be produced by gas behind shock fronts. However, in order to produce Hα emission which is not broader than what is readily resolvable by Fabry Perot observations, the gas will have to have cooled somewhat behind the shock, and it is very difficult to prevent prohibitively large H I column densities from building up (§ 3.3). We considered the properties of partial isothermal gas spheres in quasi-hydrostatic equilibrium with and without dark matter. Assuming the ionization is set by photoionization from the metagalactic UV background radiation, we find that the structures are very large unless the central neutral hydrogen column density is much larger than the ray along which we happen to view 3C 273 and/or unless substantial dark matter is present. We obtained improved data covering the region where the C IV counterparts to the two Lyα absorbers should be found, and estimate upper limits to the C IV column density in these two systems of $\sim 2 \times 10^{13}$ cm^{-2}. Without knowledge of the ionization parameter we are unable to say for certain whether the C abundance is below the solar value, but plausible guesses at the structure of the clouds and the radiation fields suggest that the C/H ratio is probably less than about one-fourth solar (§ 5).

Further attempts to observe Hα emission associated with low-redshift Lyα clouds are of interest. They should be carried out in such a way that they can distinguish between emission from irregular structure, such as might be expected from incipient star formation, as opposed to diffuse and moderately uniform surface brightness, since, as we have shown, the latter imposes constraints on the Lyα clouds and their environments which are difficult to understand. In addition to such Hα surface brightness measurements a firm detection (or improved lower limit) on the metagalactic background radiation field away from the vicinity of normal galaxies is very much needed.

The low-redshift absorbers may have nothing to do with currently popular models for the high-redshift Lyα clouds. As emphasized recently by Lanzetta et al. (1994), a significant fraction of the low redshift Lyα absorbers may be not merely associated with, but may be literal extensions of, nearby galaxies. On the other hand, both Morris et al. (1993) and Stocke et al. (1994) have found evidence for Lyα absorbers which are so isolated as *not* to be interpretable in terms of halos of normal galaxies. Measurements of the characteristic size of low-redshift Lyα clouds along two adjacent lines of sight—both those which appear to be associated with galaxies and those which do not—would be exceedingly valuable.

We thank Jennifer Sandoval, Mike Crenshaw, and Keith Feggans at GSFC for carrying out the bulk of the reductions. We thank J. Ostriker, S. Simkin, H. Ferguson, J. Miralda-Escude, D. Cox, and R. Carswell for discussions on various aspects of this work. We are especially grateful to Ted Williams for communicating the null results of the 1994 Fabry Observations of 3C 273. R. J. W., M. R., and S. L. M. acknowledge support through NASA contract NAS 5-30101 and NSF grant AST 90-05117.

REFERENCES

Bahcall, J. N., Jannuzi, B. T., Schneider, D. P., Hartig, G. F., Bohlin, R., & Junkkarinen, V. 1991, ApJ, 377, L5
Bell, K. L., & Kingston, A. E. 1967, MNRAS, 136, 241
Bingelli, B., Sandage, A., & Tammann, G. A. 1985, AJ, 90, 1681
Biretta, J. A., Sterns, C. P., & Harris, D. E. 1991, AJ, 101, 1632
Blackwell, J. et al. 1993, A User's Guide to the GHRS Software, Version 2.1 (Greenbelt: Goddard Space Flight Center)
Brandt, J. et al. 1993, AJ, 105, 831
Burstein, D., Bertola, F., Buson, L. M., Faber, S. M., & Lauer, T. R. 1988, ApJ, 328, 440
Carswell, R. F., Webb, J. K., Baldwin, J. A., & Attwood, B. 1987, ApJ, 337, 605
Ferguson, H. C. et al. 1991, ApJ, 382, L69
Ferland, G. J. 1993, Univ. of Kentucky Dept. of Physics and Astronomy Internal Rep.
Gilliland, R., Morris, S. L., Weymann, R. J., Ebbets, D. C., & Lindler, D. J. 1992, PASP, 104, 367
Giovanelli, R., & Haynes, M. P. 1989, ApJ, 346, L5
Hogan, C. 1987, ApJ, 316, L59
Kulkarni, V. P., & Fall, S. M. 1993, ApJ, 413, L63
Lanzetta, K., Bowen, D., Tytler, D., & Webb, J. 1994, ApJ, in press
Madau, P. 1992, ApJ, 389, L1
Morris, S. L., Weymann, R. J., Savage, B. D., & Gilliland, R. L. 1991, ApJ, 377, L21
Morris, S. L., Weymann, R. J., Dressler, A., McCarthy, P., Smith, B., Terrile, R., Giovanelli, R., & Irwin, M. 1993, ApJ, 419, 524
Osterbrock, D. E. 1989, Astrophysics of Gaseous Nebulae and Active Galactic Nuclei (Mill Valley, CA: University Science Books)
Rauch, M., Weymann, R. J., & Morris, S. L. 1994, in preparation
Salzer, J. J. 1992, AJ, 103, 385
Salzer, J. J., Alighieri, S. diS., Matteucci, F., Giovanelli, R., & Haynes, M. P. 1991, AJ, 101, 1258
Sandage, A. R., Bingelli, B., & Tammann, G. A. 1985, AJ, 90, 1759
Schmutzler, T., & Tscharnuter, W. M. 1993, A&A, 273, 318
Silk, J., & Werner, M. W. 1969, ApJ, 158, 185
Smette, A., Surdej, J., Shaver, P. A., Foltz, C. B., Chaffee, F. H., Weymann, R. J., Williams, R. E., & Magain, P. 1992, ApJ, 389, 39
Stocke, J. T., Shull, J. M., Penton, S., Burks, G., & Donahue, M. 1994, poster paper presented at 1994 January Washington, DC, meeting of the AAS

Takano, S., et al. 1989, Nature, 340, 289
Tytler, D., & Fan, X.-M. 1994, ApJ, 424, L87
van Gorkom, J. H., Bahcall, J. N., Jannuzi, B. T., & Schneider, D. P. 1993, AJ, 106, 2213
Vogel, S., Weymann, R. J., Rauch, M., & Hamilton, T. 1994, ApJ, in press
Webb, J. K. 1987, Ph.D. thesis, Cambridge Univ.
Weymann, R. J. 1993, in Proc. 3d Teton Summer School, The Environment and Evolution of Galaxies, ed J. M. Shull & H. A. Thronson (Kluwer: Dordrecht), 213
Williams, T. B., & Schommer, R. A. 1993, ApJ, 419, L53 (WS93)
———. 1994, in preparation